

Published in final edited form as:

*Biomaterials*. 2014 May ; 35(14): 4382–4389. doi:10.1016/j.biomaterials.2014.01.078.

## Controlling chitosan-based encapsulation for protein and vaccine delivery

Bhanu prasanth Koppolu<sup>1</sup>, Sean G. Smith<sup>1</sup>, Sruthi Ravindranathan<sup>1</sup>, Srinivas Jayanthi<sup>2</sup>,  
Thallapuranam K.S. Kumar<sup>2</sup>, and David A. Zaharoff<sup>1</sup>

<sup>1</sup>Department of Biomedical Engineering, University of Arkansas

<sup>2</sup>Department of Chemistry and Biochemistry, University of Arkansas

### Abstract

Chitosan-based nano/microencapsulation is under increasing investigation for the delivery of drugs, biologics and vaccines. Despite widespread interest, the literature lacks a defined methodology to control chitosan particle size and drug/protein release kinetics. In this study, the effects of precipitation-coacervation formulation parameters on chitosan particle size, protein encapsulation efficiency and protein release were investigated. Chitosan particle sizes, which ranged from 300 nm to 3  $\mu$ m, were influenced by chitosan concentration, chitosan molecular weight and addition rate of precipitant salt. The composition of precipitant salt played a significant role in particle formation with upper Hofmeister series salts containing strongly hydrated anions yielding particles with a low polydispersity index (PDI) while weaker anions resulted in aggregated particles with high PDIs. Sonication power had minimal effect on mean particle size, however, it significantly reduced polydispersity. Protein loading efficiencies in chitosan nano/microparticles, which ranged from 14.3% to 99.2%, was inversely related to the hydration strength of precipitant salts, protein molecular weight and directly related to the concentration and molecular weight of chitosan. Protein release rates increased with particle size and were generally inversely related to protein molecular weight. This study demonstrates that chitosan nano/microparticles with high protein loading efficiencies can be engineered with well-defined sizes and controllable release kinetics through manipulation of specific formulation parameters.

### 1. Introduction

Chitosan is under investigation for a wide variety of biomedical applications including drug delivery, gene delivery, wound healing, antimicrobial applications, tissue engineering and vaccine delivery [1-6]. The use of chitosan in these diverse applications is supported by its exceptional versatility. Chitosan can be used in solutions, hydrogels and/or nano/microparticles, while an endless array of chitosan derivatives with customized biochemical properties can be prepared through facile conjugation of side chain moieties to solvent-accessible amine and hydroxyl groups. As a result, chitosan is currently among the most well-studied biomaterials; nearly 2000 publications in the biomedical literature used chitosan as a keyword in 2013. For reference, other ubiquitous biomaterials, polylactic-co-

© 2014 Elsevier Ltd. All rights reserved.

**Corresponding author:** David A. Zaharoff, Ph.D. 120 John A. White, Jr. Engineering Hall Fayetteville, AR 72701 Phone: (479) 575-2005 Fax: (479) 575-4346 zaharoff@uark.edu.

**Publisher's Disclaimer:** This is a PDF file of an unedited manuscript that has been accepted for publication. As a service to our customers we are providing this early version of the manuscript. The manuscript will undergo copyediting, typesetting, and review of the resulting proof before it is published in its final citable form. Please note that during the production process errors may be discovered which could affect the content, and all legal disclaimers that apply to the journal pertain.

glycolic acid (PLGA) and polycaprolactone (PCL) were keywords in less than 800 and 400 publications, respectively, last year.

Chitosan nano/microparticulate systems, in particular, are under development for facilitating the delivery of genes, protein biologics and antigens [7-12]. When developing nano/microparticulate systems for drug/protein delivery applications it is important to be able to control characteristics, such as particle size, size distribution, and surface charge, as these can significantly influence release kinetics. For example, increasing particle size has been shown to increase drug release rates of encapsulated drugs/proteins [13, 14]. In addition, particle size has been shown to influence uptake by immune cells in vaccine applications. Particles with sizes similar to pathogens, such as viruses (5-300 nm) and bacteria (1-5  $\mu\text{m}$ ), are readily taken up and processed by antigen presenting cells (APCs) which leads to enhanced vaccine responses. Our recent studies demonstrated that 1  $\mu\text{m}$  chitosan particles were optimal for uptake by both dendritic cells and macrophages, however, APC activation was highest with 300nm chitosan particles [12].

It is clear that different biomedical applications will require unique chitosan particles with well-defined dimensions and release characteristics. Thus, there exists a need to develop a methodology for effective control of chitosan particle size, protein loading efficiency and protein release. Chitosan particles have been manufactured via a variety of chemistries including cross-linking, ionotropic gelation and precipitation-coacervation [15-18]. These last two methods are particularly attractive for the delivery of labile polypeptides as encapsulation is accomplished under mild aqueous conditions.

In this study, we utilized the precipitation-coacervation technique to comprehensively characterize the effects of various formulation factors, such as chitosan concentration, precipitant salt concentration, chitosan molecular weight, rate of precipitant addition, protein size and sonication power on chitosan particle size, polydispersity, and protein loading efficiency. A range of precipitant salts with varying strengths of hydration in the Hofmeister series were explored. In vitro release studies were performed to determine the effect of particle size, precipitant salt, and encapsulated protein on protein release from chitosan nano/microparticles. An analysis of the binding between proteins and chitosan explains the impact of protein-chitosan interactions during encapsulation and release. The results obtained in this study will be useful in the standardization of protocols for the preparation of chitosan-encapsulated proteins.

## 2. Materials and Methods

### 2.1. Reagents

Chitosans with viscosities of 20, 20-200, 200-600, 600-1200, and 1200-2000 cPs, were purchased from Primex (Siglufjordur, Iceland) and purified via filtration in hydrochloric acid and precipitation in sodium hydroxide. Pluronic F-68, acetic acid, sodium chloride (NaCl), potassium chloride (KCl), sodium sulfate ( $\text{Na}_2\text{SO}_4$ ), ammonium sulfate ( $(\text{NH}_4)_2\text{SO}_4$ ), magnesium sulfate ( $\text{MgSO}_4$ ), potassium sulfate ( $\text{K}_2\text{SO}_4$ ), sodium citrate ( $\text{Na}_3\text{C}_6\text{H}_5\text{O}_7$ ), trisodium phosphate ( $\text{Na}_3\text{PO}_4$ ), fluorescein isothiocyanate-labeled bovine serum albumin (FITC-BSA), unlabeled BSA and ovalbumin (OVA) were purchased from Sigma (St. Louis, MO). FITC- OVA, FITC-insulin and FITC-concanavalin A (FITC-ConA) were purchased from Life Technologies (Green Island, NY).

### 2.2. Preparation and characterization of chitosan particles

Chitosan particles were prepared using the precipitation-coacervation method developed by Berthold et al. with slight modifications [19, 20]. In brief, chitosan was dissolved in a 2% (v/v) acetic acid solution. Chitosan particles were formed by adding 50 mM precipitant salt

solution drop wise to the chitosan solution using an infusion pump (Pump 11 Elite, Harvard Apparatus, Holliston, MA). Nonionic stabilizer Pluronic F-68 was added and particles were allowed to stabilize for 2 hours under constant stirring and intermittent sonication using a sonicator (S4000; Misonix Inc., Farmingdale, New York). Chitosan particles were collected after centrifugation at 25,000g for 10 min at 4°C and freeze dried (FreeZone, Labconco, Kansas City, MO) before further use. Chitosan particles loaded with various fluorescence-labeled proteins including FITC-BSA, FITC-Insulin, FITC-OVA, and FITC-ConA, were prepared in a similar manner except that proteins were dissolved in chitosan solution before adding the precipitant salt solution. Size and polydispersity index (PDI) of the resultant particles were determined by dynamic light scattering (DLS) (Zetasizer, NanoZS90, Malvern).

### 2.3. Effect of formulation factors on particle properties

The influence of formulation factors, including chitosan concentration, molecular weight, rate of precipitant addition, protein size, and sonication power, on chitosan particle size and size distribution was determined. Preliminary experiments indicated that precipitant concentration, stabilizer concentration, pH, and chitosan:protein ratio had negligible effect on chitosan particle size (data not shown). Therefore, an experimental design using 6 factors including chitosan concentration (0.5 to 5 mg/ml), chitosan viscosity (< 20 to 1200 cPs), precipitant salt composition, infusion rate of precipitant (0.2 to 8 ml/min), sonication power (0 to 40 W), and proteins of different sizes (insulin – (6 kDa), ovalbumin – (45 kDa), BSA – (66.5 kDa), and ConA – (105 kDa)) was utilized. A constant chitosan-to-protein mass ratio of 10:1 was maintained for all experiments. The experimental design is shown in Table 1.

### 2.4. Protein loading and release studies

Protein loading efficiency was calculated indirectly. Briefly, the amount of FITC-conjugated protein remaining in the supernatant after removing the protein-loaded chitosan particles was determined through spectrofluorimetry. The difference between the initial and the unencapsulated protein concentrations was divided by the initial concentration (equation 1).

$$\text{Percentage loading efficiency} = \frac{(\text{Initial conc} - \text{Unencapsulated conc})}{\text{Initial conc}} \times 100$$

For protein release studies, FITC-BSA loaded chitosan particles with discrete sizes (300 nm, 1 μm, and 3 μm) (see Table 2) and salt groups (Na<sub>2</sub>SO<sub>4</sub>, (NH<sub>4</sub>)<sub>2</sub>SO<sub>4</sub>, MgSO<sub>4</sub>, K<sub>2</sub>SO<sub>4</sub>, and Na<sub>3</sub>C<sub>6</sub>H<sub>5</sub>O<sub>7</sub>) (see Table 3) were prepared using data gathered from previous experiments. FITC-BSA loaded chitosan particles were suspended in deionized water or phosphate buffered saline (PBS) and incubated in total darkness at 37°C. To determine the effect of protein size on release profile, chitosan particles loaded with different proteins, i.e. FITC-labeled insulin, OVA, BSA, and ConA (see Table 4), were suspended in PBS and incubated at 37°C. Supernatants were collected and replaced by fresh deionized water or PBS at regular intervals for 2 weeks. Samples were stored in the dark at –20°C until batch analysis on a spectrofluorometer (excitation wavelength: 490 nm, emission wavelength: 540 nm). Percent protein released was determined by dividing the amount of released protein by total encapsulated protein. For all release studies, the starting amount of encapsulated protein was fixed at 100μg for all groups.

### 2.5. Isothermal Titration Calorimetry

The interactions of chitosan (average molecular weight = 96kDa) with BSA and OVA in deionized water with NaCl concentrations ranging from 0 to 100 μM were studied via isothermal calorimetry. Titration experiments were performed using a Microcal VP-ITC

calorimeter (Northampton, MA) at 25 °C, with a stirring speed of 300 rpm, and 240 seconds of spacing between each 10 µl injection. In all cases, 29 injections of the 40 µM protein solution were titrated into the 1.4 ml cell containing chitosan solution at a concentration of 100 nM (0.0096 mg/ml). A protein-to-buffer blank was subtracted from the raw data to account for heats of dilution. The raw data were fit to a single-site binding model using Origin 7.0 (OriginLab, Northampton, MA) to obtain a curve fit and determine the thermodynamics parameters for each interaction. Every titration that exhibited significant binding was repeated at least three times.

## 2.6. Statistical Analysis

All experiments were carried out in triplicate or quadruplicate. Where appropriate, data are presented as means ± standard deviation. Where indicated, analysis of variance (ANOVA) was performed using JMP software (SAS, Cary, NC). Statistical significance was accepted at the  $p < 0.05$  level.

## 3. Results

### 3.1. Effect of precipitant salt type on chitosan particle properties

Preliminary studies indicated that salt concentration, surfactant (Pluronic F-68) concentration, and chitosan:protein ratio had negligible effect on chitosan particle size, polydispersity and encapsulation efficiency (data not shown). Therefore, subsequent experiments focused on other factors such as chitosan concentration, chitosan molecular weight, precipitant salt composition, precipitant salt addition rate, sonication power, and protein size. The viscosity of chitosan was used as a surrogate for molecular weight as the two properties are related [21] and molecular weight of polydisperse chitosan is not often reported.

To isolate the effect of precipitant salt composition, all other formulation parameters were fixed. Chitosan concentration was kept at 1 mg/ml, chitosan viscosity was 200-600 cPs, precipitant salt concentration was 100 mM, precipitant salt addition rate was 8 ml/min, sonication power was maintained at 10 W, and FITC-BSA was used as a model protein.

Salts with anions and cations of varying hydration strength, according to the Hofmeister series, were utilized. Sodium was used as a cationic constant while the effect of anion type was explored. Likewise, sulfate was used as anionic constant while the effect of cation type was investigated. As seen in Table 1, decreasing the hydrating strength of anionic component of precipitant salt affected particle size. Specifically, sulfate and citrate anions with high degrees of hydration induced the formation of  $427 \pm 5.5$  nm to  $490 \pm 18.3$  nm particles, respectively. As the degree of hydration was reduced, through the phosphates, particle size increased from  $427 \pm 5.5$  nm to  $1621 \pm 188$  nm. A further reduction in hydration strength to chloride anions was not able to form particles. Changing the cationic component of the salt had less of an effect on particle size with sulfate salts of magnesium, sodium, and ammonium producing  $445 \pm 7.7$  nm,  $427 \pm 7.6$  nm, and  $550 \pm 3.5$  nm particles, respectively. In general, the PDI for all particles formed was between 0.11 to 0.15 except when  $\text{Na}_3\text{PO}_4$  was used and PDI increased to 0.66.

Increasing the hydration strength of the anionic component from phosphate to sulfate to citrate resulted in marked increases in protein loading efficiencies from  $14.68 \pm 1.7\%$  to  $54 \pm 2.6\%$  to  $83.7 \pm 3.5\%$ , respectively. Once again, changing the cationic component of the salt did not significantly influence the protein loading efficiency. In fact, sulfate salts of sodium, ammonium, and magnesium produced chitosan particles with protein loading efficiencies of  $54 \pm 2.6\%$ ,  $62.5 \pm 6.1\%$ , and  $47.5 \pm 2.0\%$ , respectively.

### 3.2. Effect of chitosan molecular weight and concentration on chitosan particle properties

To isolate the effect of the chitosan molecular weight, Na<sub>2</sub>SO<sub>4</sub> was used as the precipitant salt and all other formulation parameters were fixed as described above. Chitosan particle size was found to be directly related to chitosan molecular weight, i.e. viscosity (Figure 1). Particle sizes more than doubled, from 418±16.2 nm to 854±26.2 nm, by increasing the intrinsic viscosity of chitosan from <20 cPs to 1200 – 2000 cPs (Table 1). In contrast, chitosan molecular weight did not significantly influence protein loading efficiencies which were between 50.4±2.3% to 58.5±4.2% (Table 1).

To isolate the effect of the chitosan concentration, chitosan with viscosity of 20-200 cPs was used, and all other formulation parameters were fixed as described above. Increasing chitosan concentration from 0.5 mg/ml to 5 mg/ml resulted in particle size increasing from 334±27.5 nm to 656±10.6 nm (Figure 1, Table 1). Protein loading efficiencies were similar for 0.5, 1.0 and 2.0 mg/ml. However, when chitosan concentration was increased to 3 and 5 mg/ml, the protein loading efficiency jumped to 73.6±2.2% and 92±0.8% respectively.

### 3.3. Effect of sonication on chitosan particle properties

To isolate the effect of sonication, Na<sub>2</sub>SO<sub>4</sub> was used as the precipitant salt and all other formulation parameters were fixed as describe above. Chitosan particles prepared using 10 W sonication decreased in size to 438±3.9 nm from 922±79.2 nm without sonication (Figure 1). PDI also decreased from 0.657 without sonication to 0.182 at 10 W (Table 1). Further increasing sonication power to 40 W did not significantly affect particle size. However, PDI was further reduced to 0.098 at 40 W (Table 1).

While increasing sonication power was effective in increasing particle uniformity, protein loading efficiency was reduced. Loading efficiencies decreased from 92.3±1.8% without sonication, to 88.3±5.3% at 10 W, to 74.2±6.3% at 20W, and 56.5±2.6% at 40 W (Table 1).

### 3.4. Effect of salt addition rate on chitosan particle properties

To isolate the effect of salt addition rate, Na<sub>2</sub>SO<sub>4</sub> was used as the precipitant salt and all other formulation parameters were fixed as described above. Precipitant salt addition rate was inversely related to chitosan particle size. Increasing the salt addition rate from 0.2 ml/min to 8 ml/min resulted in a decrease in particle size from 774±33.23 nm to 424±2.1 nm (Figure 1, Table 1). Most of the size reduction was observed in the lower range of salt addition rates. In addition to becoming smaller, particles also became more uniform as PDI was reduced from 0.580 to 0.121.

Protein loading efficiency was also inversely related to precipitant salt addition rate. Loading efficiencies decreased steadily from 71.9±7.0% at 0.2 ml/min, to 67.3±3.2 at 1 ml/min, 65.3±3.6% at 3 ml/min, 62±2.8% at 5 ml/min and 58.1±2.2% at 8 ml/min.

### 3.5. Effect of protein molecular weight on chitosan particle properties

A range of proteins, FITC-Insulin (6 kDa), FITC-OVA (45 kDa), FITC-BSA (66.5 kDa), and FITC-ConA (105 kDa) were selected to study the effect of protein size on chitosan particle properties. Na<sub>2</sub>SO<sub>4</sub> was used as the precipitant salt while all other formulation parameters were fixed as described above. The size of the encapsulated protein had no significant effect on chitosan particle size ( $p>0.05$ ). However, loading efficiencies decreased with increasing protein molecular weight. Chitosan particles were loaded with FITC-Insulin, FITC-OVA, FITC-BSA, and ConA at 98.3±0.5%, 96.5±1.1%, 58.1±2.5%, and 53.5±3.6% efficiency, respectively (Table 1). Interestingly, even though the molecular weight of OVA is similar to BSA, OVA was encapsulated by chitosan at a much higher efficiency than



BSA. This finding implies that molecular weight is not the only factor influencing encapsulation efficiency

### 3.6. Effect of release media ionic strength on protein release

Chitosan and protein molecules are expected to bind electrostatically before and after particle formation. As a result, exposure of particles to solutions with high concentrations of ions is expected to disrupt electrostatic bonds and affect protein release. To explore the effect of release media ionic strength on protein release, FITC-BSA encapsulated chitosan particles formulated with  $\text{Na}_2\text{SO}_4$  with mean size of  $448 \pm 12$  nm and protein loading of  $56.4 \pm 6.3\%$  were exposed to increasing concentrations of PBS. Indeed, FITC-BSA release increased with ionic strength of the releasing media. Particles incubated in 0.1X, 0.5X, and 1X PBS released 34.2%, 39.7%, and 45.2% of encapsulated FITC-BSA over a 1 week period (Figure 2). In contrast, particles incubated with deionized water released only 2.6% of encapsulated protein.

### 3.7. Effect of chitosan particle size on protein release

To study the influence of particle size on protein release, FITC-BSA encapsulated chitosan particles with nominal sizes of 300 nm, 1  $\mu\text{m}$ , and 3  $\mu\text{m}$  were generated based on the results of Table 1. The actual particle sizes were  $318.2 \pm 11$  nm,  $1133 \pm 54.1$  nm, and  $2871 \pm 216$  nm (Table 2). FITC-BSA loading efficiencies were  $58.1 \pm 3.7\%$ ,  $83.5 \pm 8.3\%$ , and  $96.6 \pm 0.6\%$ , respectively.

As seen in Figure 3, FITC-BSA release profiles from all particle sizes were characterized by an initial burst of about 5-10% of the encapsulated protein followed by a slow, sustained release in which a total of 30-50% of the protein was released in PBS over 1 week. The amount of FITC-BSA released increased with increasing particle size. The “300 nm,” “1  $\mu\text{m}$ ,” and “3  $\mu\text{m}$ ” groups released 31.4%, 42.6%, and 46.9% of their encapsulated FITC-BSA within one week.

### 3.8. Effect of precipitant salt on protein release

FITC-BSA encapsulated chitosan particles formulated with  $\text{Na}_2\text{SO}_4$ ,  $(\text{NH}_4)_2\text{SO}_4$ ,  $\text{MgSO}_4$ ,  $\text{Na}_3\text{C}_6\text{H}_5\text{O}_7$ , and  $\text{Na}_3\text{PO}_4$  yielded particles of sizes  $448 \pm 12$  nm,  $561 \pm 3.4$  nm,  $462 \pm 6.3$  nm,  $478 \pm 64.3$  nm, and  $1423 \pm 156$  nm respectively, with protein loading efficiency of  $56.4 \pm 6.3\%$ ,  $62 \pm 5.3\%$ ,  $54.3 \pm 3.4\%$ ,  $86 \pm 2.1\%$ , and  $14.3 \pm 6.6\%$ , respectively (Table 3).

Protein release profiles of particles were dependent on the cationic component of precipitant salt with total amount protein release decreasing with decreasing hydrating strength of cations.  $\text{MgSO}_4$ ,  $\text{Na}_2\text{SO}_4$ , and  $(\text{NH}_4)_2\text{SO}_4$  particles released 50.87%, 45.2%, and 31.7% respectively over one week (Figure 4). However, changing the anion of the salt caused significant change in protein release profile of the particles with  $\text{Na}_3\text{C}_6\text{H}_5\text{O}_7$ ,  $\text{Na}_2\text{SO}_4$ , and  $\text{Na}_3\text{PO}_4$  particles releasing 51.4%, 45.2%, and 98.1% of encapsulated protein over one week (Figure 4).

### 3.9. Effect of encapsulated protein on protein release

Chitosan particles precipitated with  $\text{Na}_2\text{SO}_4$  and loaded with FITC-insulin, FITC-OVA, FITC-BSA, and FITC-ConA were similarly sized at  $421 \pm 10.1$  nm,  $429 \pm 3.6$  nm,  $448 \pm 22.4$  nm, and  $452 \pm 5$  nm, respectively (Table 4). Protein loading efficiencies varied as before (Table 1) at  $99.2 \pm 0.1\%$ ,  $98 \pm 0.4\%$ ,  $56.4 \pm 3.2\%$ , and  $53.4 \pm 1.8\%$ , respectively.

As shown in Figure 5, the nature of encapsulated protein had a significant effect on release kinetics. The two largest proteins, FITC-BSA and FITC-ConA, exhibited the highest levels of burst and cumulative release, 48.2% and 48.9%, respectively, over a one week period

(Figure 5). The smallest protein, FITC-insulin, exhibited very little burst release but reached 40.42% release over one week. Interestingly, the vast majority of FITC-OVA remained in chitosan particles after one week with only 2.4% released. Even though OVA and BSA are similar in size, OVA has a lower isoelectric point (pI) and therefore a higher negative surface charge under particle formulation conditions facilitating increased electrostatic interactions with polycationic chitosan.

### 3.10. Chitosan-protein binding in solution

ITC was used to investigate the binding interactions of chitosan with model proteins. Titrations were performed at pH 6.5, where OVA (pI=4.5) and BSA (pI=5.3) both possess a net negative charge while chitosan is highly cationic. Both OVA and BSA bound strongly to chitosan via exothermic interactions in deionized water, i.e. 0 mM NaCl solution (Figure 6). The interaction between OVA and chitosan, with a binding constant ( $K_a$ ) of  $3.5 \times 10^7 \pm 9.4 \times 10^6 \text{ M}^{-1}$ , was stronger than that of BSA and chitosan where  $K_a$  was  $1.1 \times 10^6 \pm 1.6 \times 10^5 \text{ M}^{-1}$  (Table 5). OVA bound less strongly in the presence of 10 mM NaCl ( $K_a = 6.8 \times 10^6 \pm 1.4 \times 10^6 \text{ M}^{-1}$ ) and not at all in 25 mM NaCl or 100 mM NaCl. The binding stoichiometry of chitosan to OVA and chitosan to BSA is 1:17 and 1:12, respectively.

## 4. Discussion

There are several published methods for manufacturing drug or protein-loaded chitosan particles [15-18]. Methods include the use of crosslinking agents [16, 22, 23], emulsion-precipitation [24], ionotropic gelation and precipitation-coacervation. The use of crosslinkers or organic solvents during emulsion-precipitation can be detrimental when encapsulating labile proteins. While both precipitation-coacervation and ionotropic gelation can form chitosan particles in mild aqueous conditions, precipitation-coacervation was preferred for two reasons. First, based on our own experiences, as well as published data, the size of chitosan particles generated via ionotropic gelation is restricted to less than  $1 \mu\text{m}$  [23, 24]. Second, ionotropic gelation generally results in lower drug/protein loading efficiencies with 38-72% of BSA loading efficiencies observed with ionotropic gelation compared to 74-98% obtained with precipitation coacervation method [7, 25].

In this study, we comprehensively explored the effects of 10 precipitation-coacervation parameters on chitosan particle size, polydispersity, protein loading efficiency and protein release. Four of the 10 parameters were eliminated in preliminary studies as having no impact. The remaining 6 factors were studied individually by isolating a single parameter while fixing the other 5 parameters.

Chitosan particle size was found to increase with chitosan concentration and molecular weight/viscosity and decreased with precipitant salt addition rate and sonication power. The effect of chitosan concentration and molecular weight can be explained by the fact that addition of increased amounts of the chitosan starting material to the precipitation-coacervation reaction increases the probability of interaction of chitosan polymers to form larger particles. Conversely, a higher salt addition rate reduced chitosan-chitosan and chitosan-protein interactions and led to the formation of smaller sized particles. The effect of sonication was consistent with published studies demonstrating that chitosan particles prepared through ionotropic gelation were reduced in both size and PDI after sonication [26, 27]. Our data indicate that a threshold level of sonication is preferred to produce a more uniform size distribution of chitosan particles, but that further increases in sonication power adversely affected loading efficiency.

Protein loading efficiencies increased with chitosan concentration and molecular weight/viscosity. These findings were consistent with previous studies demonstrating that drug

loading and release from chitosan particles was directly related to chitosan molecular weight/viscosity [28]. Higher chitosan molecular weight and/or concentration increases the likelihood of anionic proteins interacting with cationic chitosan molecules prior to precipitation.

In general, protein loading efficiencies decreased as protein molecular weight increased. However, we also identified protein charge as a major factor in loading efficiency. The isoelectric points for the four encapsulated proteins are similar with the exception of OVA (Table 4). With the lowest pI, OVA carried the strongest negative surface charge during encapsulation and release. Our findings that protein release increased with ionic strength of the releasing media (Figure 2) and that NaCl disrupts protein-chitosan binding (Table 5) indicate that protein-chitosan binding is mediated via electrostatic interactions. Therefore, a highly negatively charged protein, such as OVA, will be loaded in cationic chitosan particles more efficiently and released more slowly than a similarly sized protein with a more neutral or positive net charge.

Among the strongest effects on chitosan-protein particle formation was the hydration strength of precipitant salt anions. Strong Hofmeister series anions with high degrees of hydration, such as citrate and sulfate, induced formation of smaller and more uniform particles. Decreasing the degree of hydration by using phosphate anions resulted in an increase in both particle size and polydispersity likely due to particle aggregation of weakly formed particles. A further decrease down the Hofmeister classification to chloride anions abrogated particle formation. These results were expected as salts with strongly hydrated ions can strip away water molecules from proteins or biopolymers resulting in salting out or precipitation [29, 30]. Weaker ions such as  $\text{Cl}^-$  are unable to remove a sufficient amount of water to induce precipitation.

Interestingly, strong Hofmeister anions also induced higher loading efficiencies. It was originally predicted that strong anions would independently disrupt chitosan-protein binding and precipitate chitosan and protein. However, it appears that mixing chitosan and protein prior to addition of precipitant salt allows sufficient electrostatic binding for the chitosan-protein complexes to salt out together. Taken together with our particle size analysis, in general, strong Hofmeister anions were better at forming highly loaded, chitosan-protein particles.

Release studies demonstrated that protein release from chitosan particles, regardless of the sample group was characterized by an initial burst followed by sustained release. The release was found to be strongly dependent on the releasing medium with 34.1-45.2% protein release observed in PBS compared to that of 2.6% observed in deionized water. While previous studies showed that the release of drug from chitosan particles was dependent on solution pH [25, 31], our studies show that the release is also dependent on the ionic strength of the medium. ITC studies showed that chitosan-protein binding was dependent on the salinity of solution. Specifically, chitosan-protein interaction was significant at 0mM NaCl, but was eliminated at 25 mM NaCl. In mildly acidic aqueous solutions, chitosan's primary amines are protonated. Thus, polycationic chitosan molecules interact electrostatically with co-formulated proteins. These positive charges are likely to be responsible for electrostatic interactions with proteins. However, when high levels of free anions, such as chlorides and phosphates, are present, they can interact with the protonated chitosan and disrupt protein binding resulting in lower loading efficiencies and/or faster release rates [19, 32].

Overall, smaller proteins were released from chitosan particles much more quickly. However, OVA, despite being similar in size to BSA, was a notable exception. Only 2.4%



of OVA was released compared to 48.1% of BSA. This discrepancy can be explained by the higher binding constant and free energy change of OVA versus BSA (Table 5). In general, proteins with higher densities of negative surface charges are likely to be loaded in chitosan particles more efficiently and released more slowly. We are currently investigating the effects of a protein's charge density on its interactions with chitosan and other polysaccharides.

Finally, protein release rate was found to increase with particle size. Whether this effect is driven by pore size, which we believe increases with particle size, is the subject of future studies. Nevertheless, these data imply that one can customize protein release profiles through manipulation of chitosan particle size.

## 5. Conclusion

Protein-encapsulated chitosan particles are under exploration for a variety of biomedical applications. Each application is likely to require unique chitosan particles with specific dimensions and release characteristics. Until now, it was not clear how to reproducibly manufacture protein-encapsulated chitosan nano/microparticles with high loading efficiencies. The results of this study demonstrate that the properties of chitosan particles including size, size distribution, protein loading and release can be effectively modulated by controlling a handful of precipitation-coacervation formulation parameters. Understanding the influence of these parameters will help standardize chitosan particle-based delivery for continued preclinical and clinical development. Furthermore, the included protocols provide a useful roadmap for the development of unique chitosan nano/microparticles for customized delivery of protein biologics and vaccines.

## Acknowledgments

This work was supported by the National Cancer Institute (K22CA131567 to D.A.Z.).

## References

- [1]. Kas HS. Chitosan: properties, preparations and application to microparticulate systems. *J Microencapsul.* 1997; 14:689–711. [PubMed: 9394251]
- [2]. Sinha VR, Singla AK, Wadhawan S, Kaushik R, Kumria R, Bansal K, et al. Chitosan microspheres as a potential carrier for drugs. *Int J Pharm.* 2004; 274:1–33. [PubMed: 15072779]
- [3]. Chandy T, Sharma CP. Chitosan as a biomaterial. *Biomater Artif Cells Artif Organs.* 1990; 18:1–24. [PubMed: 2185854]
- [4]. Chandy T, Sharma CP. Chitosan matrix for oral sustained delivery of ampicillin. *Biomaterials.* 1993; 14:939–44. [PubMed: 8268386]
- [5]. Mao HQ, Roy K, Troung-Le VL, Janes KA, Lin KY, Wang Y, et al. Chitosan-DNA nanoparticles as gene carriers: synthesis, characterization and transfection efficiency. *J Control Release.* 2001; 70:399–421. [PubMed: 11182210]
- [6]. Janes KA, Fresneau MP, Marazuela A, Fabra A, Alonso M, J. Chitosan nanoparticles as delivery systems for doxorubicin. *J Control Release.* 2001; 73:255–67. [PubMed: 11516503]
- [7]. Gan Q, Wang T. Chitosan nanoparticle as protein delivery carrier--Systematic examination of fabrication conditions for efficient loading and release. *Colloids and Surfaces B: Biointerfaces.* 2007; 59:24–34.
- [8]. Xu Y, Du Y. Effect of molecular structure of chitosan on protein delivery properties of chitosan nanoparticles. *Int J Pharm.* 2003; 250:215–26. [PubMed: 12480287]
- [9]. Nagamoto T, Hattori Y, Takayama K, Maitani Y. Novel chitosan particles and chitosan-coated emulsions inducing immune response via intranasal vaccine delivery. *Pharm Res.* 2004; 21:671–4. [PubMed: 15139524]

- [10]. Seferian PG, Martinez ML. Immune stimulating activity of two new chitosan containing adjuvant formulations. *Vaccine*. 2000; 19:661–8. [PubMed: 11090719]
- [11]. Zaharoff DA, Rogers CJ, Hance KW, Schlom J, Greiner JW. Chitosan solution enhances both humoral and cell-mediated immune responses to subcutaneous vaccination. *Vaccine*. 2007; 25:2085–94. [PubMed: 17258843]
- [12]. Koppolu B, Zaharoff DA. The effect of antigen encapsulation in chitosan particles on uptake, activation and presentation by antigen presenting cells. *Biomaterials*. 2013; 34:2359–69. [PubMed: 23274070]
- [13]. Lim ST, Martin GP, Berry DJ, Brown MB. Preparation and evaluation of the in vitro drug release properties and mucoadhesion of novel microspheres of hyaluronic acid and chitosan. *J Control Release*. 2000; 66:281–92. [PubMed: 10742587]
- [14]. Siepmann J, Faisant N, Akiki J, Richard J, Benoit JP. Effect of the size of biodegradable microparticles on drug release: experiment and theory. *J Control Release*. 2004; 96:123–34. [PubMed: 15063035]
- [15]. Bugamelli F, Raggi MA, Orienti I, Zecchi V. Controlled insulin release from chitosan microparticles. *Archiv der Pharmazie*. 1998; 331:133–8. [PubMed: 9648521]
- [16]. Ko JA, Park HJ, Hwang SJ, Park JB, Lee JS. Preparation and characterization of chitosan microparticles intended for controlled drug delivery. *Int J Pharm*. 2002; 249:165–74. [PubMed: 12433445]
- [17]. van der Lubben IM, Verhoef JC, van Aelst AC, Borchard G, Junginger HE. Chitosan microparticles for oral vaccination: preparation, characterization and preliminary in vivo uptake studies in murine Peyer's patches. *Biomaterials*. 2001; 22:687–94. [PubMed: 11246962]
- [18]. Huang Y, Yeh M, Chiang C. Formulation factors in preparing BTM-chitosan microspheres by spray drying method. *Int J Pharm*. 2002; 242:239–42. [PubMed: 12176254]
- [19]. Berthold A, Cremer K, Kreuter J. Preparation and characterization of chitosan microspheres as drug carrier for prednisolone sodium phosphate as model for anti-inflammatory drugs. *J Control Release*. 1996; 39:17–25.
- [20]. Gordon S, Saupe A, McBurney W, Rades T, Hook S. Comparison of chitosan nanoparticles and chitosan hydrogels for vaccine delivery. *J Pharm Pharmacol*. 2008; 60:1591–600. [PubMed: 19000363]
- [21]. Terbojevich M, Cosani A, Muzzarelli RAA. Molecular parameters of chitosans depolymerized with the aid of papain. *Carbohydr Polym*. 1996; 29:63–8.
- [22]. Hu B, Pan C, Sun Y, Hou Z, Ye H, Zeng X. Optimization of fabrication parameters to produce chitosan-tripolyphosphate nanoparticles for delivery of tea catechins. *J Agric Food Chem*. 2008; 56:7451–8. [PubMed: 18627163]
- [23]. Gan Q, Wang T, Cochrane C, McCarron P. Modulation of surface charge, particle size and morphological properties of chitosan-TPP nanoparticles intended for gene delivery. *Colloids Surf B Biointerfaces*. 2005; 44:65–73. [PubMed: 16024239]
- [24]. Kobiasi MA, Chua BY, Tonkin D, Jackson DC, Mainwaring DE. Control of size dispersity of chitosan biopolymer microparticles and nanoparticles to influence vaccine trafficking and cell uptake. *J Biomed Mater Res A*. 100A:1859–67.
- [25]. Ozbas-Turan S, Akbuga J, Aral C. Controlled release of interleukin-2 from chitosan microspheres. *J Pharm Sci*. 2002; 91:1245–51. [PubMed: 11977100]
- [26]. Pan Y, Li YJ, Zhao HY, Zheng JM, Xu H, Wei G, et al. Bioadhesive polysaccharide in protein delivery system: chitosan nanoparticles improve the intestinal absorption of insulin in vivo. *Int J Pharm*. 2002; 249:139–47. [PubMed: 12433442]
- [27]. Tang ES, Huang M, Lim LY. Ultrasonication of chitosan and chitosan nanoparticles. *Int J Pharm*. 2003; 265:103–14. [PubMed: 14522123]
- [28]. Genta I, Perugini P, Pavanetto F. Different molecular weight chitosan microspheres: influence on drug loading and drug release. *Drug Dev Ind Pharm*. 1998; 24:779–84. [PubMed: 9876526]
- [29]. Cacace MG, Landau EM, Ramsden JJ. The Hofmeister series: salt and solvent effects on interfacial phenomena. *Q Rev Biophys*. 1997; 30:241–77. [PubMed: 9394422]

- [30]. Record MT Jr, Guinn E, Pegram L, Capp M. Introductory lecture: interpreting and predicting Hofmeister salt ion and solute effects on biopolymer and model processes using the solute partitioning model. *Faraday Discuss.* 2013; 160:9–44. discussion 103–20. [PubMed: 23795491]
- [31]. Tokumitsu H, Ichikawa H, Fukumori Y. Chitosan-gadopentetic acid complex nanoparticles for gadolinium neutron-capture therapy of cancer: preparation by novel emulsion-droplet coalescence technique and characterization. *Pharm Res.* 1999; 16:1830–5. [PubMed: 10644070]
- [32]. Chang KLB, Lin J. Swelling behavior and the release of protein from chitosan pectin composite particles. *Carbohydr Polym.* 2000; 43:163–9.

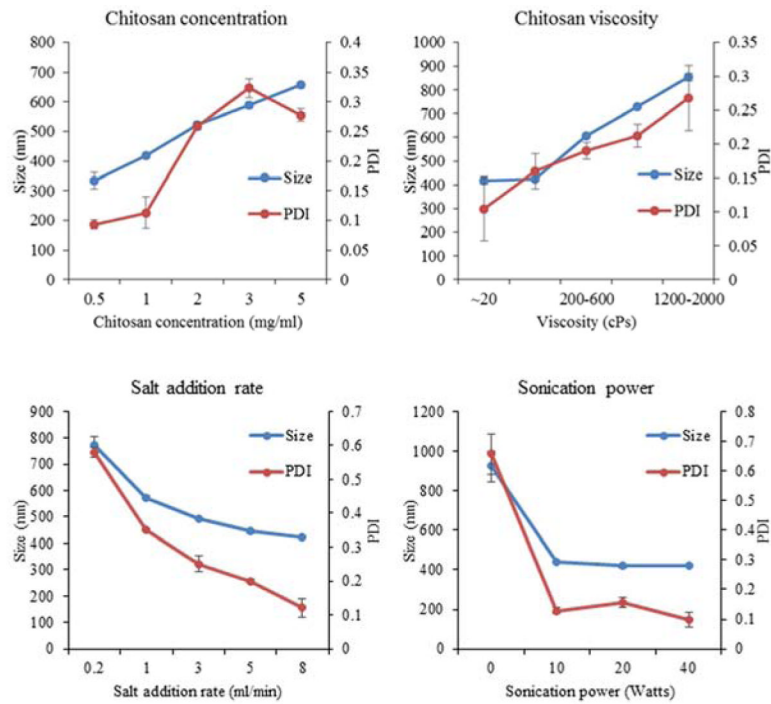


**Fig. 1.** Effect of precipitation-coacervation parameters on chitosan-FITC-BSA particle size and PDI. Parameters including: chitosan concentration, molecular weight/viscosity, precipitant salt addition rate, and sonication power were varied following the experimental design described in Table 1. Resultant particle size and PDI of the resultant particles were determined by DLS. Data are presented as mean  $\pm$  standard deviation of three independent experiments.

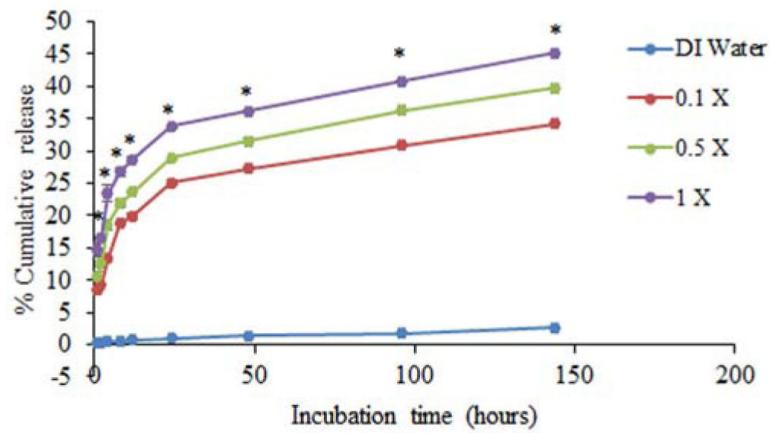


**Fig. 2.** Effect of ionic strength of release media on protein release. Chitosan particles containing 100 $\mu$ g of the model protein FITC-BSA were prepared using Na<sub>2</sub>SO<sub>4</sub> and incubated with deionized water (DI water), 0.1X, 0.5X or 1 X PBS. Samples were collected at each time point and protein release was quantified by measuring fluorescence using a spectrofluorometer. Each data point represent the mean of 4 independent samples. Particles incubated in any amount of PBS showed significantly higher protein release ( $P < 0.05$ ) than particles in DI water at all time points. \*indicates a statistically significant difference in cumulative release among the different PBS groups ( $P < 0.05$ ).



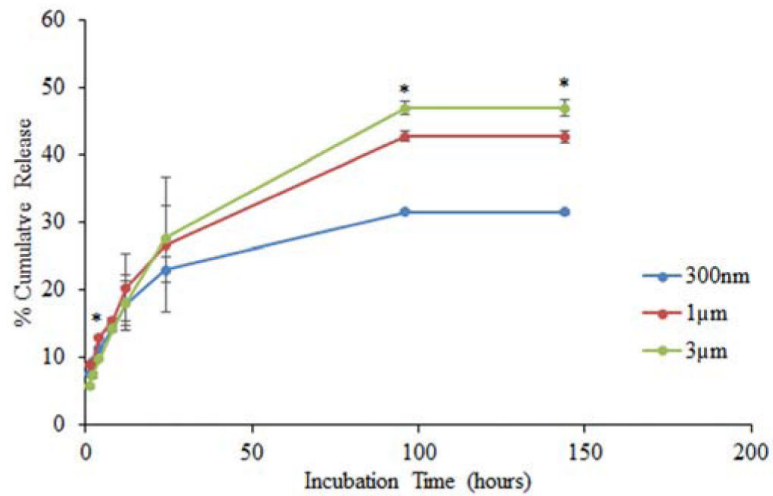


**Fig. 3.** Effect of chitosan particle size on protein release. 300nm, 1 µm, and 3 µm chitosan particles encapsulating 100µg FITC-BSA were incubated with PBS. Samples were collected at each time point and protein release was quantified by measuring fluorescence using spectrofluorometer. Each data point represents the mean of 4 independent samples. \* indicates a statistically significant difference in cumulative release among the different chitosan particle sizes ( $P < 0.05$ ).

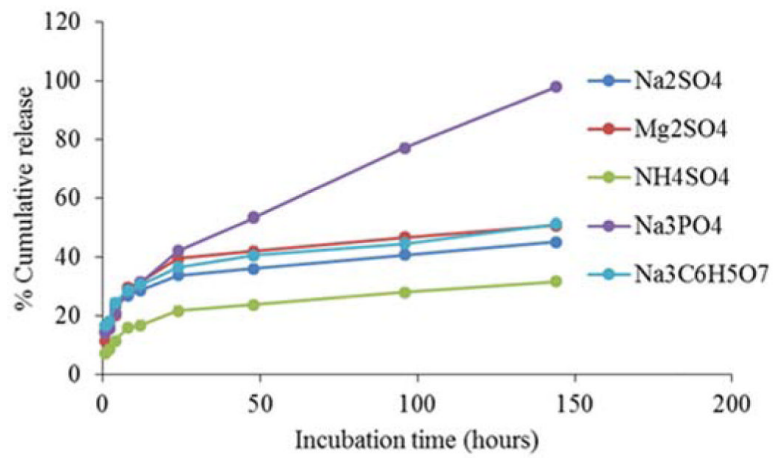


**Fig. 4.**

Effect of hydration strength of precipitating salt on protein release. Chitosan particles containing 100 $\mu$ g FITC-BSA were prepared using Hofmeister series salts: Na<sub>2</sub>SO<sub>4</sub>, (NH<sub>4</sub>)<sub>2</sub>SO<sub>4</sub>, MgSO<sub>4</sub>, Na<sub>3</sub>C<sub>6</sub>H<sub>5</sub>O<sub>7</sub>, or Na<sub>3</sub>PO<sub>4</sub>, and released in PBS. Samples were collected at each time point and protein release was quantified by measuring fluorescence using a spectrofluorometer. Each data point represents the mean of 4 independent samples. Protein release by NH<sub>4</sub>SO<sub>4</sub> particles was significantly lower than other precipitant salt groups at all time points ( $P < 0.05$ ). Protein release by Na<sub>2</sub>SO<sub>4</sub> particles was significantly lower than other precipitant salt groups for incubation times greater than 48 hours ( $P < 0.05$ ).

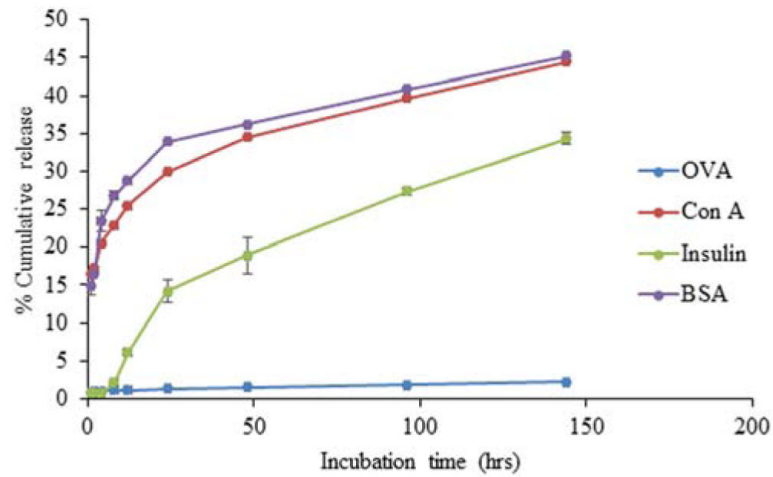


**Fig. 5.** Effect of encapsulated protein size on protein release. Chitosan particles encapsulating 100 $\mu$ g of model proteins FITC-Insulin, FITC-OVA, FITC-BSA, and FITC-ConA were incubated in PBS. Samples were collected at each time point and protein release was quantified by measuring fluorescence using a spectrophotometer. Each data point represents the mean of 4 independent samples. BSA and ConA release was significantly higher than that of Insulin and OVA at all time points ( $P < 0.05$ ). Insulin release was significantly higher than that of OVA at incubation times greater than 2 hours ( $P < 0.05$ ).

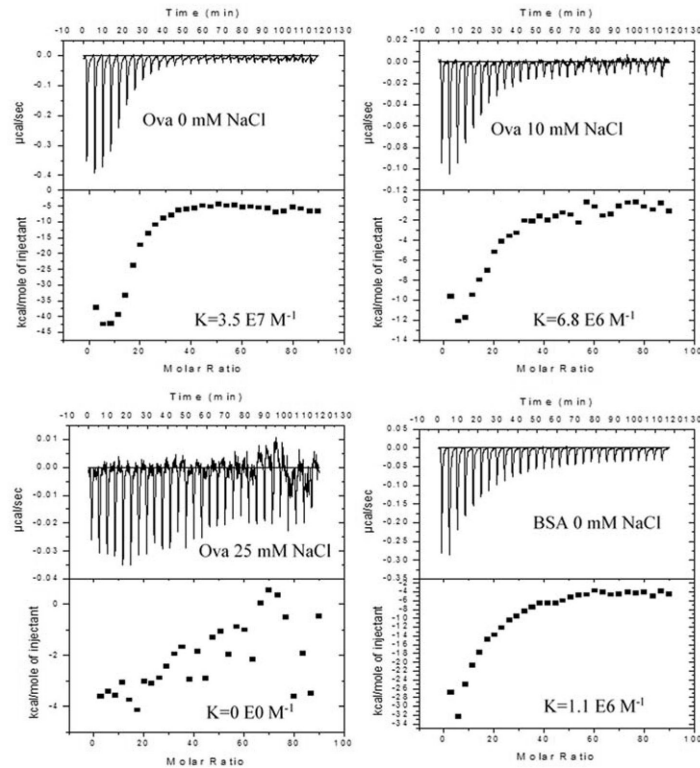


**Fig. 6.** Effect of protein type and salt concentration on protein-chitosan binding. Isothermal titration calorimetry of ovalbumin (OVA) and bovine serum albumin (BSA) into chitosan indicates differences in reactions dependent upon the protein and salt concentration. The top panel of each figure shows the raw heats per injection with each peak representing a single injection. The lower panel shows the integrated total enthalpy per mole of injectant as a function of the molar ratio of the protein to the chitosan with each point representing a single injection. BSA or OVA solutions were titrated into chitosan in deionized water, 10 or 25mM NaCl as indicated. All titrations were performed at a pH of 6.5 and 25 °C using Microcal's VP-ITC with 100 nM chitosan in the cell and 40 M protein in the syringe.

**Table 1**

Effect of formulation factors on particle size, size distribution and protein loading efficiency.

Parameter	Level	Mean Size (nm)	PDI	Protein loading efficiency (%)
Precipitant salt	Na <sub>3</sub> C <sub>6</sub> H <sub>5</sub> O <sub>7</sub>	490 ± 18.3	0.154	83.7 ± 3.5
	Na <sub>2</sub> SO <sub>4</sub>	427 ± 7.6	0.113	54 ± 2.6
	Na <sub>3</sub> PO <sub>4</sub>	1621 ± 188.0	0.667	14.6 ± 1.7
	NaCl	-*	-	-
	KCl	-*	-	-
	MgSO <sub>4</sub>	445 ± 7.7	0.124	47.5 ± 2.0
	(NH <sub>4</sub> ) <sub>2</sub> SO <sub>4</sub>	551.9 ± 3.5	0.135	62.5 ± 6.1
Chitosan Viscosity <sup>a</sup> (molecular weight)	<20 cPs	418 ± 16.2	0.104	50.3 ± 2.3
	20-200 cPs	424 ± 7.7	0.160	56.5 ± 3.4
	200-600 cPs	605 ± 13.3	0.190	56.5 ± 2.6
	600-1200 cPs	728 ± 15.0	0.212	53.5 ± 4.3
	1200-2000 cPs	854 ± 26.2	0.385	58.5 ± 4.2
Chitosan Concentration	0.5 mg/ml	334 ± 27.5	0.093	58.5 ± 3.4
	1 mg/ml	418 ± 3.5	0.113	57.3 ± 2.5
	2 mg/ml	521 ± 2.8	0.259	59.9 ± 6.8
	3 mg/ml	587 ± 10.6	0.182	73.6 ± 2.2
	5 mg/ml	656 ± 13.6	0.277	92 ± 0.8
Sonication power	0 W	922 ± 79.2	0.657	92.3 ± 1.8
	10 W	438 ± 3.9	0.182	88.3 ± 5.3
	20 W	418 ± 9.6	0.156	74.2 ± 6.3
	40 W	421 ± 4.1	0.098	56.5 ± 2.6
Precipitant salt addition rate	0.2 ml/min	774 ± 33.2	0.580	71.9 ± 7.0
	1 ml/min	574 ± 9.1	0.350	67.3 ± 3.2
	3 ml/min	495 ± 3.6	0.250	65.3 ± 3.6
	5 ml/min	444 ± 5.6	0.200	62 ± 2.8
	8 ml/min	424 ± 2.1	0.121	58.1 ± 2.2
Protein	Insulin	411 ± 19.3	0.195	98.3 ± 0.5
	Ova	423 ± 3.6	0.178	96.5 ± 1.1
	BSA	424 ± 7.7	0.160	58.1 ± 2.5
	Con A	410 ± 5.5	0.113	53.5 ± 3.6

<sup>a</sup> viscosity range of chitosan was indicated by the manufacturer as obtained at a concentration of 1 mg/ml (w/v) in 1% acetic acid<sup>b</sup> no particles formed



**Table 2**

Experimental design for protein release studies: Effect of particle size

Nominal size	Chitosan conc.	Precipitant salt	Protein	Salt addition rate	Actual Mean Size (nm)	Protein loading efficiency (%)
300nm	0.5 mg/ml	Na <sub>2</sub> SO <sub>4</sub>	FITC-BSA	8 ml/min	318.2±11	58.1±3.7
1µm	3 mg/ml	Na <sub>2</sub> SO <sub>4</sub>	FITC-BSA	1 ml/min	1133±54.1	83.5±8.3
3µm	5 mg/ml	Na <sub>2</sub> SO <sub>4</sub>	FITC-BSA	0.2 ml/min	2871±216	96.6±0.6

**Table 3**

Experimental design for protein release studies: Effect of precipitant salt composition

Precipitant salt	Chitosan conc	Protein	Salt addition rate	Mean Size (nm)	Protein loading efficiency (%)
Na <sub>2</sub> SO <sub>4</sub>	1 mg/ml	FITC-BSA	8 ml/min	448±12	56.4±6.3
(NH <sub>4</sub> ) <sub>2</sub> SO <sub>4</sub>	1 mg/ml	FITC-BSA	8 ml/min	561±3.4	62±5.3
MgSO <sub>4</sub>	1 mg/ml	FITC-BSA	8 ml/min	462±6.3	54.3±3.4
Na <sub>3</sub> C <sub>6</sub> H <sub>5</sub> O <sub>7</sub>	1 mg/ml	FITC-BSA	8 ml/min	478±64.3	86±2.1
Na <sub>3</sub> PO <sub>4</sub>	1 mg/ml	FITC-BSA	8 ml/min	1423±156	14.3±6.6

**Table 4**

Experimental design for protein release studies: Effect of protein molecular weight

Protein	Molecular weight	pI	Chitosan conc	Precipitant salt	Salt addition rate	Mean Size (nm)	Protein loading efficiency (%)
Insulin	6 kDa	5.3	1 mg/ml	Na <sub>2</sub> SO <sub>4</sub>	8 ml/min	421±10.1	99.2±0.1
OVA	45 kDa	4.5	1 mg/ml	Na <sub>2</sub> SO <sub>4</sub>	8 ml/min	429±3.6	98±0.4
BSA	66.5 kDa	5.3	1 mg/ml	Na <sub>2</sub> SO <sub>4</sub>	8 ml/min	448±22.4	56.4±3.2
Con A	105 kDa	5.4	1 mg/ml	Na <sub>2</sub> SO <sub>4</sub>	8 ml/min	452±5	53.4±1.8

**Table 5**

Thermodynamic parameters generated from isothermal titration calorimetry experiments.

Protein	NaCl conc. (mM)	K ( $M^{-1}$ )	$\Delta H$ (cal/mol)	$\Delta S$ (cal/mol $\cdot^{\circ}K$ )	$\Delta G$ (cal/mol)
OVA	0	$3.5 \times 10^7 \pm 9.4 \times 10^6$	$3.4 \times 10^4 \pm 3.9 \times 10^3$	$8.1 \times 10^1 \pm 1.3 \times 10^1$	$1.0 \times 10^4 \pm 1.3 \times 10^2$
OVA	10	$6.8 \times 10^6 \pm 1.4 \times 10^6$	$1.1 \times 10^4 \pm 3.1 \times 10^2$	$7.1 \times 10^0 \pm 1.4 \times 10^0$	$9.3 \times 10^3 \pm 1.1 \times 10^2$
OVA	25	0	0	0	0
OVA	100	0	0	0	0
BSA	0	$1.1 \times 10^6 \pm 1.6 \times 10^5$	$5.6 \times 10^4 \pm 1.8 \times 10^3$	$1.6 \times 10^2 \pm 6.2 \times 10^0$	$8.1 \times 10^3 \pm 9.2 \times 10^1$